J Seismol (2021) 25:339–345
https://doi.org/10.1007/s10950-020-09980-x

SHORT COMMUNICATION

Calculation of extreme accelerations in earthquake motion due to ground spalling

Igor A. Beresnev

Received: 2 December 2019 / Accepted: 22 December 2020 / Published online: 7 January 2021

Abstract The occurrence of record-breaking extreme vertical acceleration, caused by the separation of the loosely attached ground and its subsequent landing, was discovered during the 2008 M_w 6.9 Iwate-Miyagi earthquake in Japan. The phenomenon was termed the trampoline effect and later referred to as spalling. The trampoline model is quantitatively inaccurate, as it assumes a soft elastic rebound, whereas large accelerations could only be produced by hard collision. We present a computational model of spalling based on Hertz's theory of solid impact and the projectile equation. It quantitatively reproduces the asymmetric shape of the acceleration time history, in which the negative phase is capped at one negative gravity, and the observed high values in the positive slapdown phase. The model predicts that the ground spalling can increase the maximum possible acceleration that can be experienced in an earthquake to seven gravities. Such a scenario should be taken into account in seismic-hazard analyses.

Keywords Extreme ground motions · Ground spalling · Slapdown phase

I. A. Beresnev (✉)
Department of Geological & Atmospheric Sciences, Iowa State University, 253 Science I, 2237 Osborn Drive, Ames, IA 50011-3212, USA
e-mail: beresnev@iastate.edu

1 Introduction

Following the 2008 M_w 6.9 Iwate-Miyagi earthquake in Japan, a phenomenon was reported in which part of the near-surface ground temporarily separated from the underlying rocks, was thrown into the air, and underwent a period of free fall, producing sharp acceleration spikes upon landing. The process led to a characteristic asymmetric shape of the resulting ground-acceleration time history with respect to the horizontal axis (Aoi et al. 2008). The phenomenon was coined the trampoline effect. The unprecedented large vertical ground accelerations of nearly 4 g in the spikes (g being the acceleration of gravity) resulted. Although the report was the first observation of its kind during an earthquake, the same effects, known as spalling, were experimentally and theoretically investigated, including theoretical analyses of the resulting stress and strain, in the near field of underground nuclear explosions (Eisler and Chilton 1964; Chilton et al. 1966; Eisler et al. 1966). Following the earlier established terminology, the sharp positive acceleration spikes were referred to as the "slapdown" phases by Yamada et al. (2009).

Similar asymmetry in two vertical-component acceleration traces at the surface was recently reported during the 2018 M_w 6.6 Hokkaido eastern Iburi event (Dhakal et al. 2019, figure 9a). The peak accelerations in these records were approximately 1.1 and 1.6 g. The occurrence of asymmetry was accompanied by the classic manifestations of nonlinear-elastic behavior of near-surface materials, such as the reduction in high-frequency amplification and shift in the site resonance to lower frequencies.

Although the trampoline analogy introduced by Aoi et al. (2008) correctly captures the formation of sign asymmetry (positive vs. negative pulses) in ground accelerations in a qualitative way, the model cannot accurately predict the magnitude of the sharp positive spikes resulting from spalling. The explanation is that a trampoline, due to its elastic nature, softens the impact of a falling body, while the spikes are produced by it hitting a hard surface. The difference is illustrated by the fact that, for example, in the vein of the same analogy, a person falling off a roof of a multi-story building and landing on a trampoline may experience a few bounces but will generally be safe, whereas the landing on hard ground will most probably be lethal.

A quantitative model of the spalling phenomenon should therefore necessarily involve a hard impact. Such a model enables the prediction of the earthquake hazard caused by the possibility of ground separation and the extreme accelerations that follow. It also supplies the values of the greatest accelerations possible during an earthquake due to a combination of regular earthquake loading and ground spalling.

2 The model of ground spalling

Our model is the one of a mass lying on a rigid vertically vibrating platform. Let the vertical position of the platform and the mass be u and U, respectively, and the relative displacement of the mass $U_1 = U - u$. The positive direction of the vertical axis is upward. Suppose the mass is at rest on the surface of the platform, and at a certain time its vertical vibration begins. The time history $u(t)$ of the vibration is given. The task is to calculate $U(t)$.

In the beginning, as long as the condition $\ddot{u} \geq -g$ is satisfied ($g = 9.8$ m/s^2), the mass remains in contact with the platform, and $\ddot{U} = \ddot{u}$. We refer to this case as cohesion. When the condition becomes violated, separation (spalling) occurs, and the mass is thrown into the air. Then, its displacement is described by the projectile equation:

$$U = u_0 + \dot{u}_0 t - g t^2/2, \tag{1}$$

where u_0 and $\dot{u}_0$ are the initial values of the displacement and velocity imparted by the platform at the moment of separation. The mass remains in the air, with constant acceleration of $\ddot{U} = -g$, as long as the condition $U_1 > 0$ holds. At the moment of impact, U_1 turns to zero. At that moment, the hard hit occurs, and the mass acquires the velocity of the platform. A positive acceleration spike (the slapdown phase) is produced, equal to $\ddot{U} = \left(\dot{u} - \dot{U}\right)/\tau$, where $\dot{u}$ and $\dot{U}$ are the velocities of the platform and the falling mass at the instant of the impact, respectively, and τ is the period of time over which the impact takes place. This formula considers the impact to be instantaneous in the sense that the interval Δt, at which the values are sampled in the resulting acceleration time history, is greater than τ. The validity of this assumption will be verified. Following the impact, the cohesion condition holds again, and the process is repeated. The flow chart, illustrating the algorithm of obtaining the full time history of $\ddot{U}$, is shown in Fig. 1.

The model neglects the repeated bounces of the mass as it hits the surface. This is a key difference between the effects of the trampoline and that of the hard surface. As one can experience by dropping a chunk of rock onto the ground, the rock will not tend to rebound in any noticeable manner. That is why our assumption is justified.

To calculate the duration of the impact τ, Hertz's theory of collision of two deforming solid bodies can be utilized. A closed-form solution is available for the case of two equal spheres impinging on each other (Love 1944, Article 140, eq. 71):

$$\tau = 2.9432 \left[\frac{25\pi^2}{8} \frac{(1-\sigma)^4}{(1-2\sigma)^2} \right]^{1/5} \frac{r}{\dot{U}_1^{1/5} V^{4/5}}, \tag{2}$$

where r is the radius of the sphere, σ is the Poisson's ratio of the sphere material, and V is its P-wave velocity. In the following, we take σ of the standard Poisson solid, $\sigma = 0.25$. The top 34 m of the profile at the station IWTH25, which underwent the spalling during the Iwate-Miyagi earthquake, were composed of river-terrace deposits with a representative P-wave velocity $V = 2000$ m/s (Aoi et al. 2008, figure S1). It is hypothesized that the ground separation occurred somewhere within this layer, and this velocity value will also be subsequently assumed. The dependences on σ and $\dot{U}_1$ in eq. (2) are very weak. The main variable controlling the value of τ is the radius. For the problem at hand, considering the separation of a ground layer composed

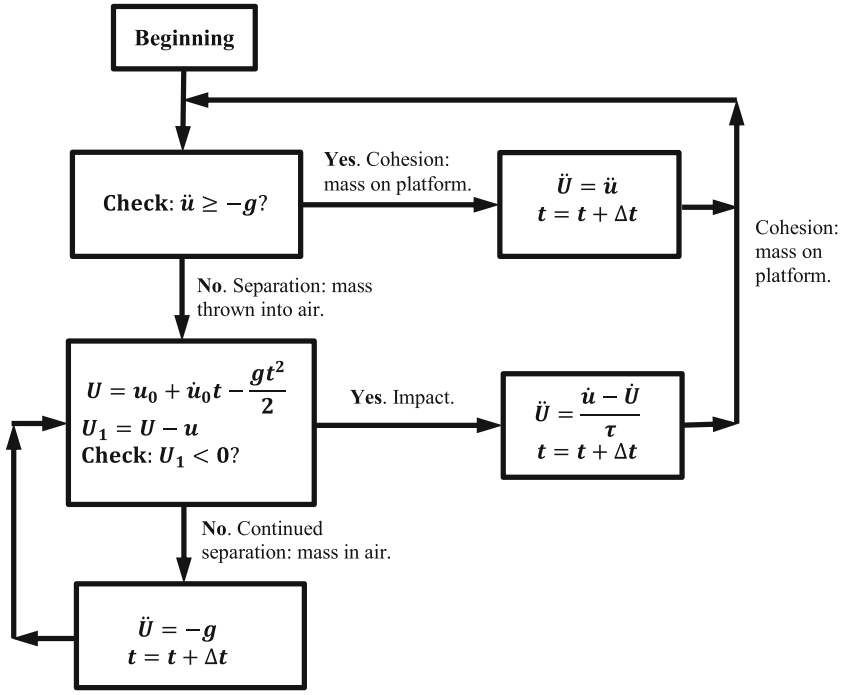

Fig. 1 Flow chart illustrating the calculation of the acceleration of the mass lying on a vertically vibrating platform

of multiple grains of unknown variable sizes from its substrate, r should be treated as an effective radius to be determined from compliance with the data. For $r =$ 0.1 m and the values of $\dot{U}_1$ on the order of 10^{-2} m/s, both obtained from running the simulations of the spalling effect at station IWTH25, eq. (2) yields $\tau = 3.5 \times 10^{-3}$ s. The sampling interval Δt of the IWTH25 accelerograms is 10^{-2} s. The condition of instantaneous impact, $\tau < \Delta t$, observed by the field instruments that recorded the earthquake, is thus satisfied.

Figure 2 illustrates the application of the algorithm of Fig. 1 to an example problem, in which the platform oscillation is pure sinusoidal with the frequency of 20 Hz, characteristic of near-field high-frequency earthquake motions, and with the acceleration amplitude of 1.2 g. The resulting acceleration $\ddot{U}$ of the mass, in units of g, is presented as a function of time. The appearance of the slapdown phases, the restriction of the negative acceleration to $-g$, and the resulting asymmetry of the accelerogram are clearly seen.

3 Application to the Iwate-Miyagi earthquake

There are two sensors at IWTH25: one at the surface and one at the depth of 260 m in a borehole (Aoi et al. 2008), which are part of the KiK-net observation network. To apply the model to reproducing the recording of the surface instrument, the input acceleration, representing the vibration of the underlying rigid platform unaffected by the spalling, is required. One can obtain the respective time history by propagating the recorded motion at 260 m to the surface using the transfer function of the intervening stack of strata. At station IWTH25, there are seven layers, with the thicknesses and P- and S-wave velocities available from borehole logging (Aoi et al. 2008, figure S1). The rock densities were assigned by us through the Gardner's rule (Sheriff and Geldart 1995, equation 5.15). The constant quality factor of $Q = 30$ in the entire section was assumed. The complex Fourier

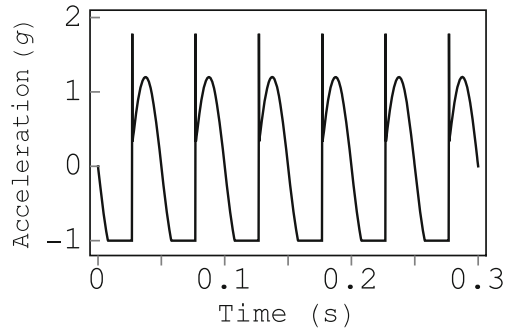

Fig. 2 The acceleration of the mass lying on a sinusoidally vibrating platform

spectrum of the input acceleration was obtained from the spectrum observed at 260 m by multiplying the latter by the spectral ratio T_0/T_{260}, where T_0 and T_{260} are the theoretical frequency-domain transfer functions of the stack at the receiver depths of zero and 260 m. The complex transfer functions were calculated using the reflection/transmission matrix method of Kennett and Kerry (1979), for the vertical component of an *S*-wave incident from below. The input accelerogram was then calculated by inverting its Fourier spectrum.

Figure 1 of Aoi et al. (2008) shows that the site IWTH25 was located above an extended rupture plane, 3 km from the epicenter and 7 km of vertical distance from the fault. Under such a geometry, waves arrive to the station at various angles. The angle of incidence of the wave impinging on the stack from below is a parameter of the transfer function and needs to be specified. To determine its most plausible effective value responsible for the radiation, we calculated the modulus of the theoretical spectral ratio T_0/T_{260} for a number of the angles of incidence ranging from 10° to 60°. These ratios were compared with the observed average one obtained by Aoi et al. (2008, figure S4) for the vertical component of a series of aftershocks. The angle of incidence of 25° provided the best fit and was chosen to represent the transfer function.

Figure 3 shows the steps involved in the process of simulating the recorded surface acceleration at station IWTH25. Going from the bottom to the top, Fig. 3d is the observed vertical record at 260 m. Figure 3c, labeled as simulated rigid ground, is the record at 260 m theoretically propagated to the surface using the procedure described. It represents the vibration $\ddot{u}$ of the rigid substrate serving as input to the ground mass loosely attached to it. Figure 3b is the resulting simulated ground acceleration $\ddot{U}$ obtained, as Fig. 2, via the algorithm of Fig. 1 to represent the ground spalling. Finally, Fig. 3a is the observed vertical surface acceleration at IWTH25.

As eq. (1) explains, knowledge of the rigid substrate displacement and velocity, as input to the loosely attached ground, is required, in addition to acceleration to calculate the resulting mass displacement U during the period of free fall. The quantities u and $\dot{u}$ were obtained from $\ddot{u}$ in Fig. 3b by single and double integration, respectively. They are shown in Fig. 4.

For realistic ground, the representative radius r of its contact roughness appearing in eq. (2) is effectively a

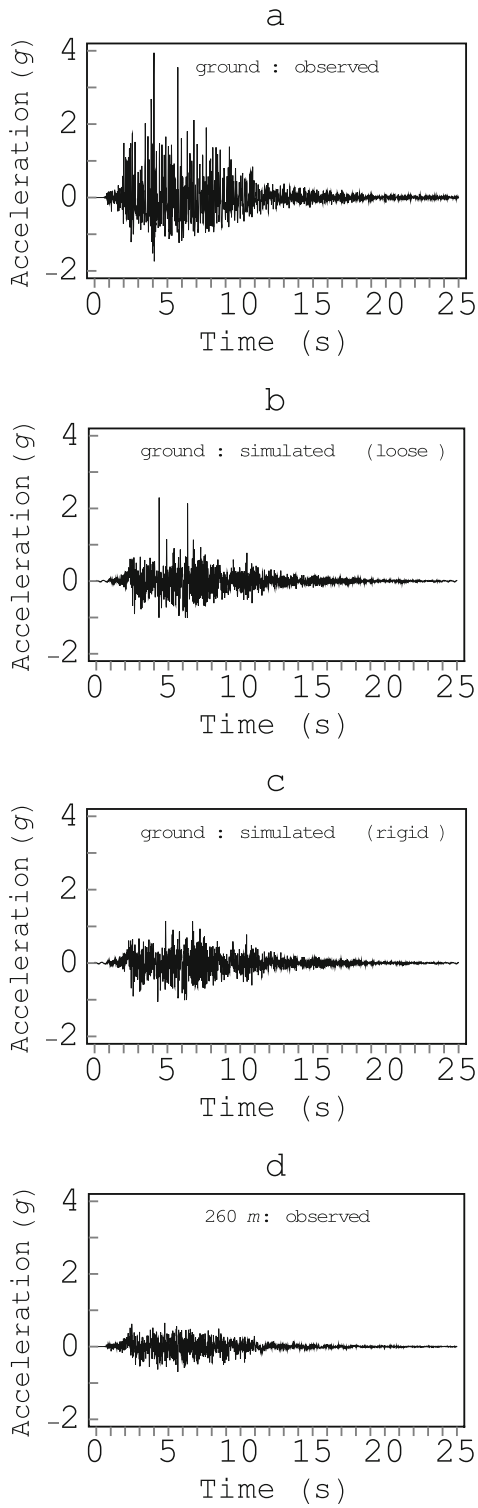

Fig. 3 Steps involved in the simulation of the observed acceleration time history at the surface of site IWTH25. **a** Ground: observed; **b** Ground: simulated (loose); **c** Ground: simulated (rigid); **d** 260 m: observed

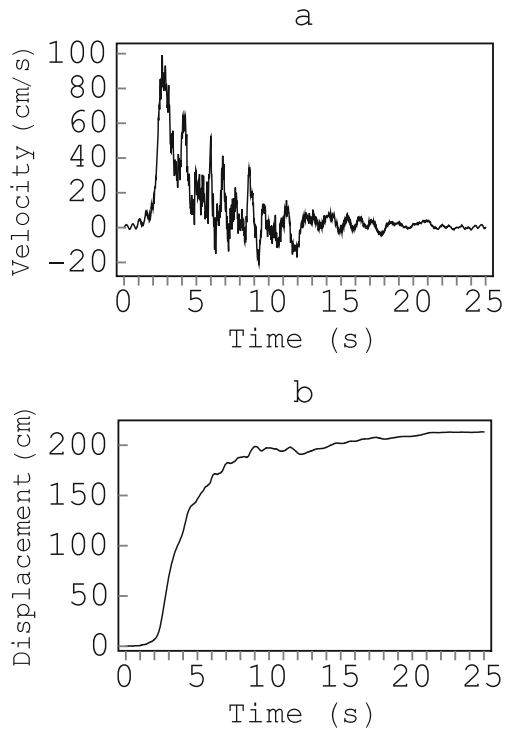

Fig. 4 Velocity (**a**) and displacement (**b**) serving as input to the ground loosely attached to the surface of an oscillating rigid substrate

free model parameter that can be established by compliance with the data. The value of $r = 0.1$ m was arrived at by trying to match the simulated peak accelerations in Fig. 3b with the observed ones in Fig. 3a. It should be noted that, by fine-tuning r to a fractional value, an exact fit can readily be obtained. We deliberately avoided this temptation, keeping r as generic as possible. The resulting mismatch between the observed and simulated values of the first (greatest) spike seen in Fig. 3a and b is a factor of 1.7.

4 Discussion

Comparison of Fig. 3a and b shows that the quantitative model of Fig. 1 is able to reproduce the transformation of the incoming seismic motion by ground spalling. Relative to the input to the softer ground seen in Fig. 3c, the acceleration time history in Fig. 3b develops the spikes of the slapdown phase and acquires the characteristic asymmetric shape, agreeing closely with the form of the observed accelerogram in Fig. 3a.

One may notice that the observed trace, albeit showing a tendency toward exhibiting a limit on the negative acceleration of $-g$, corresponding to free fall, exceeded it in one instance around 4 s. The theoretical trace is strictly capped at $-g$. This difference is to be expected. The theoretical model of the mass lying loosely on a rigid surface possesses zero tensile strength at their contact. The reality is more complex. Parts of the ground in the IWTH25 river deposits, initially completely losing cohesion and thrown upwards, as the accelerogram in Fig. 3a suggests, may have regained some tensile strength upon landing, although such a behavior is nonetheless seen an exception rather than the norm. Apart from that observation, the quantitative model of spalling correctly describes the formation of asymmetry and the generation of spikes of exceptionally large positive accelerations at the IWTH25 station.

The relative separation of the rigid substrate and the loose ground does not need to be significant to explain the high accelerations. The maximum relative separation U_1, obtained from the computation, is only 0.02 mm.

Tobita et al. (2010) considered a different conceptual model of the origin of the same observed sign asymmetry. The model does not involve ground separation but invokes differential elastic moduli in compression and tension characteristic of granular media. The asymmetry follows but does not require free fall and hard collision. Note that this model supports negative accelerations well below $-g$ (Tobita et al. 2010, p. 1461) and hence does not acknowledge the fact that the observed extreme negative vertical accelerations tend to have a lower bound of about $-1\ g$ (Yamada et al. 2009). In Tobita et al.'s simulation of the IWTH25 record, the computed accelerogram acquires a quasi-sinusoidal shape not seen in the observation (Tobita et al. 2010, figures 12d and e). Also, the simulations produced the asymmetry not only in the vertical but also in the horizontal component; the latter was not seen in the record either (cf. figures 12a and b).

A question naturally arises whether ground spalling during earthquakes can cause vertical accelerations even in excess of the record-breaking 3.9 g recorded at the surface of IWTH25. From Fig. 3c, the peak acceleration of the incoming motion, incident upon loose ground at IWTH25, was 1.1 g. On the other hand, accelerations of up to 2 g have been already documented on hard rock (Anderson 2010, table 3). Based on computations using the representation theorem of elasticity, Beresnev

(2021) estimated the maximum possible accelerations on bedrock to be saturating at the level of approximately 3 *g*. If the input trace of Fig. 3c is scaled to the peak value of 3 *g*, the resulting acceleration time history of the ground, obtained by the spalling model, is presented in Fig. 5. A pronounced sign asymmetry takes place, and, relative to Fig. 3a and b, numerous positive spikes of the ground hitting the rigid substrate occur, each causing extremely high acceleration. The peak value is 3.9 *g*, but, with the "correction factor" of 1.7, it is 6.6 *g*. This acceleration is what could have been observed at the surface of IWTH25 due to a combination of the maximum possible input loading predicted for an earthquake and the spalling of soft ground. The value of approximately 7 *g* is thus an expected all-time maximum of ground acceleration that could be observed in an earthquake under the worst-case scenario. The spalling model allows making such a quantitative prediction, which should be taken into account in seismic-hazard assessment.

Soil-structure interaction has also been proposed as a possible cause of the extreme values in vertical ground accelerations, as an alternative to true ground motion. Goto et al. (2019) considered separation of the foundation slab, on which the accelerometer was installed, from the ground surface, rather than the ground spalling, to be the real reason for the observed sign asymmetry and the resulting extreme accelerations. Our model of lifting and hard collision is not specific to the separation within the ground and equally applies to the impact of the slab against an uneven ground surface.

Aoi et al. (2008) call attention to the fact that the focus usually is on horizontal motions as the most significant component controlling the seismic load on buildings, while the contribution of the vertical motions has been undervalued. The spalling effect clearly enhances the hazard posed by the vertical component. Our paper presents the tool to quantitatively evaluate the vertical accelerations caused by the spalling, with the algorithm implementing the calculation presented in Fig. 1. The still incompletely resolved uncertainty is in the value of the representative radius *r* of the contact heterogeneity that controls the duration of the impact according to eq. (2). The values of this parameter can be derived from modeling the ground-acceleration records where clear asymmetry between the negative and positive phases in the vertical component has been established.

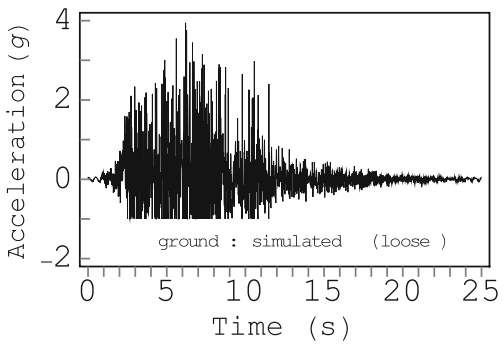

Fig. 5 The hypothetical simulated acceleration time history at the surface of IWTH25 (equivalent of Fig. 3b) obtained if the input accelerogram (Fig. 3c) is scaled to peak acceleration of 3 *g*

5 Data and resources

The KiK-net surface and borehole acceleration time histories from the Iwate-Miyagi earthquake at the IWTH25 site were downloaded from the National Research Institute for Earth Science and Disaster Resilience (Japan) (www.kik.bosai.go.jp; last accessed October 2020).

Acknowledgments The transfer functions were calculated using the FORTRAN code written by J.-C. Gariel and kindly supplied by E. Field. The author is indebted to two anonymous reviewers for their constructive comments.

References

Anderson JG (2010) Source and site characteristics of earthquakes that have caused exceptional ground accelerations and velocities. Bull Seism Soc Am 100:1–36

Aoi S, Kunugi T, Fujiwara H (2008) Trampoline effect in extreme ground motion. Science 322:727–730

Beresnev IA (2021) The strongest possible earthquake ground motion. J Earthquake Eng. https://doi.org/10.1080/13632469.2019.1691681

Chilton F, Eisler JD, Heubach HG (1966) Dynamics of spalling of the Earth's surface caused by underground explosions. J Geophys Res 71:5911–5919

Dhakal YP, Kunugi T, Kimura T, Suzuki W, Aoi S (2019) Peak ground motions and characteristics of nonlinear site response during the 2018 Mw 6.6 Hokkaido eastern Iburi earthquake. *Earth, Planets Space* **71**:56

Eisler JD, Chilton F (1964) Spalling of the Earth's surface by underground nuclear explosions. J Geophys Res 69:5285–5293

Eisler JD, Chilton F, Sauer FM (1966) Multiple subsurface spalling by underground nuclear explosions. J Geophys Res 71:3923–3927

Goto H, Kaneko Y, Young J, Avery H, Damiano L (2019) Extreme accelerations during earthquakes caused by elastic flapping effect. Sci Rep 9:1117

Kennett BLN, Kerry NJ (1979) Seismic waves in a stratified half space. Geophys J R Astron Soc 57:557–583

Love AEH (1944) A treatise on the mathematical theory of elasticity, Fourth edn. Dover Publications, New York

Sheriff RE, Geldart LP (1995) Exploration seismology, Second edn. Cambridge University Press, Cambridge

Tobita T, Iai S, Iwata T (2010) Numerical analysis of near-field asymmetric vertical motion. Bull Seism Soc Am 100:1456–1469

Yamada M, Mori J, Heaton T (2009) The slapdown phase in high-acceleration records of large earthquakes. Seismol Res Lett 80:559–564